

PROPERTIES OF CAST MAR-M-247 FOR TURBINE BLISK APPLICATIONS

Murray Kaufman

Thomson Laboratory
General Electric Company
Lynn, Massachusetts 01910
USA

Summary

The following mechanical properties of specimens cut from turbine blade/disk (blisk) castings of Mar-M-247 alloy are presented: tensile (smooth and notched), creep/rupture, high cycle fatigue, low cycle fatigue and crack growth rate. Results of an extensive search for the presence of defects in the blisk castings are reported

Introduction

Production of a turbine blade/disk rotor (blisk) as a one piece casting would offer a significant cost reduction compared to the conventional cast blade-dovetail-wrought disk rotor, as well as avoiding certain stress problems caused by the dovetail type of blade attachment. In the past, alloy and casting technology could not produce dimensionally accurate, sound castings, of adequate mechanical properties, particularly for the disk portion of the casting for application in high performance turbines in competition with conventional rotors. Cast nickel base superalloys have long established usage as turbine blades, but their disk area temperature tensile and fatigue properties are considerably lower than the better forged disk alloys, in part due to the much coarser grain size of the castings in the thicker sections of a disk.

A recent improvement in casting technology is the Grainex^(R) process of Howmet Turbine Components Corp.(1) for producing fine grains in thick sections. Combined with the capability of Hot Isostatic Pressing (HIP) to close internal porosities, it seems possible now to use castings in high performance blisk applications.

Of the various potential alloys for cast blisks, Mar-M-247 appears to have good castability, adequate strength levels and there is some structural information available (1-5). The purpose of the present work is to provide some basic mechanical properties, including smooth and notch tensile, creep-rupture, low and high cycle fatigue and crack growth rate on specimens cut from actual blisks, Grainex^(R) cast and HIP'd with the parameters established for production. In addition, because modern design methods use defect tolerance analysis, it is essential to obtain some measure of the distribution of defects, such as non-metallic inclusions and remaining porosity in actual castings. Both inspection of metallographic sections and test bar fracture surfaces are included.

Materials and Test Conditions

All material for testing in this program was obtained from a group of 14 Mar-M-247 blisks cast by the Grainex^(R) process, HIP'd at 2165F, 25 Ksi for 4 hours and heat treated at 2165F, 2 hours, plus 1600F, 20 hours by Howmet Turbine Components Corp., Austenal LaPorte Division. Five different cast configurations were involved, all with disk diameters of about 6", solid centers with hub thicknesses of about 2½" and web thicknesses of 0.6 to 0.75". Four master heats were represented (at least 2 blisks from each heat), 2 different HIP runs, and several different heat treat lots. Table I shows the chemical compositions of each of the 4 heats involved. Note that 4 different master melt sources are involved. Compositions are within the requirements for the alloy.

Specimens were cut from the blisks in the radial and tangential orientation (no axial bars). Smooth tensile and creep rupture bars had ½" dia. X 1" long gage sections. Notched tensile bars had ½" minimum dia. with a $K_t=2.8$ notch. Fatigue test bars used a cylindrical gage section, 0.2" dia.; ¾" long for LCF and ½" long for HCF testing. Crack growth specimens were of the compact tensile type, ½" thick and ~1.85" square.

Tensile tests were run at R.T., 400, 1000, 1200, 1400, 1600, 1800 and 1900F for smooth bars and R.T., 1000 and 1400F for notched bars (2 or 3 at each temperature). Creep rupture tests were run at 1400, 1600 and 1800F (3 or 4 per temperature). Crack growth tests were performed at $A=0.95$, in duplicate, at 1000 and 1400F. Both low cycle fatigue (LCF) and high

Table I. Composition of Mar-M-247 Heats

(Weight %)

Element	L11-WWS Cert. Alloy Prod.	L11-WLK Cannon- Muskegon	L11-WLB Special Metals	L11-WST Howmet Dover
Al	5.57	5.50	5.55	5.42
Ti	1.09	1.00	.95	1.03
Co	10.05	10.15	10.10	10.00
Cr	8.51	8.63	8.51	8.40
Mo	.71	.73	.77	.78
W	9.87	9.67	9.65	10.00
Ta	2.99	3.00	2.91	2.90
Hf	1.55	1.40	1.47	1.41
Fe	.16	.04	.04	.08
C	.14	.17	.17	.13
B	.016	.013	.015	.015
Zr	.03	.04	.04	.03
Si	<.1	<.05	<.05	<.05
Mn	<.1	<.05	<.05	<.05
S	.0002	.0004	.0004	.0005
N	10 ppm	6 ppm	3 ppm	6 ppm
O	18 ppm	14 ppm	10 ppm	10 ppm
Ni	Bal.	Bal.	Bal.	Bal.

cycle fatigue (HCF) testing was performed. LCF, axial-axial, strain control, at A=1 was run at 400, 1000 and 1400F, 8 specimens each. HCF testing, axial-axial at A=∞, 0.67 and 0.25 was done at 1100 and 1700F and at A=∞ and 0.25 at 1500F, 4 to 6 specimens at each condition.

Metallographic inspection of many test bars and sections cut from the blisks was performed to examine both the microstructure and for presence of defects. All the fracture surfaces of the failed fatigue bars and some of the others were examined optically and by SEM. Any "defects" found were analyzed by X-ray energy dispersive (EDX) techniques.

Test Results

The tensile data is included in Table II. In these, and other tests, no significant differences appeared as a function of specimen orientation or blisk source; only the Heat number is reported here. Both 0.2% yield strength and ultimate tensile strength remain about constant up to 1400F, above which they decrease moderately rapidly. The ductility shows a slight rise up to 1000F, followed by the usual nickel base alloy ductility minimum near 1600F. Notched bar tensile strength is always greater than the smooth bar strength, with the notch/smooth ratios as follows:

Temperature	Notch/Smooth UTS Ratio
R.T.	1.33
1000F	1.27
1400F	1.14

Table II. Mar-M-247 Tensile Test Results

Test Temp. °F	Test Type	Spec. Heat	0.2% YS ksi	U.T.S. ksi	Elong. %	R. of A. %
R.T.	Smooth	WWS	124.7	143.4	5.9	7.1
		WLK	120.8	142.9	7.3	8.2
		WLB	126.1	142.5	6.5	9.4
	$K_t=2.8$	WWS	-	188.2	-	-
		WLK	-	196.1	-	-
		WST	-	186.3	-	-
400	Smooth	WWS	117.6	143.3	6.5	7.3
		WLK	117.9	148.4	7.4	8.5
1000	Smooth	WWS	117.7	146.0	7.9	10.9
		WLK	121.3	152.0	8.1	10.4
		WLB	116.6	143.5	6.6	9.3
	$K_t=2.8$	WST	-	188.6	-	-
		WLB	-	183.9	-	-
		WLB	-	189.7	-	-
1200	Smooth	WWS	113.6	142.6	6.9	8.9
		WWS	118.2	150.8	7.2	10.5
1400	Smooth	WWS	117.2	145.1	4.3	7.4
		WST	115.3	149.0	6.1	8.2
	$K_t=2.8$	WST	-	161.0	-	-
		WWS	-	172.9	-	-
1600	Smooth	WLK	102.2	123.7	3.2	4.6
		WWS	103.6	127.1	6.6	6.9
1800	Smooth	WST	61.2	82.7	6.4	8.6
		WLK	56.4	77.5	6.8	7.0
1900	Smooth	WLK	43.2	59.1	8.3	9.8
		WST	38.6	55.4	9.2	10.4

The creep rupture data is listed in Table III. The low ductility at 1400F precluded the possibility obtaining 1 and 2% creep times. The creep time at 1400F for the specimen from Heat WWS is higher and the elongation is lower than they should be, because of the failure outside the gage length. All the other data points seem reasonable and consistent.

Table IV contains the strain controlled LCF, $A=1$, data for 400, 800 and 1400F. All discernible fracture initiation sites were at the surface, except for the four lowest strain range failures at 1400F (see next section). Scatter was not very great. At the high strain region, life decreases with increasing temperature, while at low strain ranges there is no difference in the 400 and 800F results, with the 1400F results slightly lower.

The high cycle fatigue results for the different temperatures and A ratios are summarized in Table V. All the 1100F failures seemed to be surface

Table III. Mar-M-247 Creep Rupture Test Results

Test Temp. °F	Test Stress Ksi	Heat No.	Creep Time, hrs.			Rupture Life hrs.	Elong. %	R.A. %
			0.5%	1%	2%			
1400	90	WWS*	250	-	-	274.7	1.1	1.1
	"	WST	125	-	-	140.9	1.0	1.9
	"	WLB	183	-	-	300.2	1.5	3.4
1600	55	WWS	42	77	124	217.9	7.6	8.1
	45	WLK	309	451	628	818	5.9	7.5
	"	WWS	203	336	-	724.6	6.1	7.8
1800	25	WLB	57	88	114	126.6	5.4	5.3
	22	WLK	224	287	348	412.1	5.9	8.9
	"	WWS	139	178	214	220.8	4.0	5.3

*Failed outside gage length

Table IV. Mar-M-247 Low Cycle, Strain Controlled, A=1, Fatigue Test Results

Test Temp. °F	Heat No.	Strain Range %	Mod. of Elast. 10 ⁶ psi	Cycles to Initiate	Cycles to Failure
400	WWS	.958	30.9	~1,070	1,267
	WLB	.800	31.2	~2,100	2,646
	WWS	.666	29.9	--	5,312
	WWS	.628	30.9	~9,070	9,644
	WST	.509	30.7	13,991	16,851
	WLB	.491	29.6	~24,000	25,861
	WWS	.469	29.9	--	57,169
	WLB	.380	29.9	~138,700	145,155
	800	WLB	.994	29.3	--
WLK		.970	28.9	~630	950
WST		.834	29.7	1,084	1,604
WST		.737	29.8	2,368	2,845
WLB		.694	28.8	5,776	6,976
WLB		.546	29.9	17,600	20,400
WWS		.488	29.0	~30,000	39,790
WWS		.404	29.6	~73,460	76,429
1400	WLB	.831	25.6	190	496
	WLK	.724	24.1	~670	799
	WLK	.626	25.2	2,487	3,311
	WWS	.578	23.6	5,358	6,358
	WST	.442	25.8	13,764	26,244
	WLK	.388	26.1	~31,800	33,881
	WST	.369	25.7	--	179,224 →
	WLK	.332	26.6	~98,200	99,152

→ Test stopped, no failure

Table V. Mar-M-247 High Cycle Fatigue Test Summary

Test Temp, °F	A Ratio	Alternating Fatigue Strength @ 10 ⁷ Cycles ksi
1100	∞	32.5
	.67	29.2
	.25	22.1
1500	∞	45.0
	.25	18.8
1700	∞	36.6
	.67	25.0
	.25	13.7

initiated. Most of the 1500 and 1700F failures initiated internally, although the A=∞ fracture surfaces were generally beaten too badly to locate the initiation sites (see next section). For A=∞, there seems to be a maximum of 10⁷ cycle fatigue strength at 1500F, with the 1700F value somewhat higher than the 1100F. At A=0.67 and 0.25, there is a continual decrease with increasing temperature.

Crack growth rate test results at 1000 and 1400F show: threshold stress intensity factor $K^*=8 \text{ Ksi}\sqrt{\text{in}}$ at 1000F and about 13 at 1400F. Up to a crack growth rate (dA/dN) of 10^{-4} ($K \geq 50$), the critical stress intensity factor K_C was not reached at either temperature. At each temperature the duplicate specimens were in good agreement, with a moderate test scatter.

Metallographic and Fractographic Examination

The microstructure of the different blisks, and at various locations within the hub, web and rim regions of each blisk were relatively uniform. Maximum grain size was about 1/8". Typical structures are included in Fig. 1-3. Most noticeable, particularly in the unetched condition are the fairly common occurrence of large, elongated MC type carbides up to 10 mils long, Fig. 1. Smaller MC carbides, and occasional script-like carbides are present also. Etching reveals the usual structures for high γ' percentage alloys: eutectic nodules, coring and a fair amount of coarser γ' , Figs. 2, 3. The long time at high temperature during HIP and heat treatment, without a γ' solution treatment undoubtedly caused the coarse γ' .

Of great interest for application as blisks, is the presence and morphology of possible defects. A total of 44 samples were mounted and polished, representing cross sections of test bars, radial and tangential slices from the blisks, etc., from each of the heats supplied. The results are summarized below:

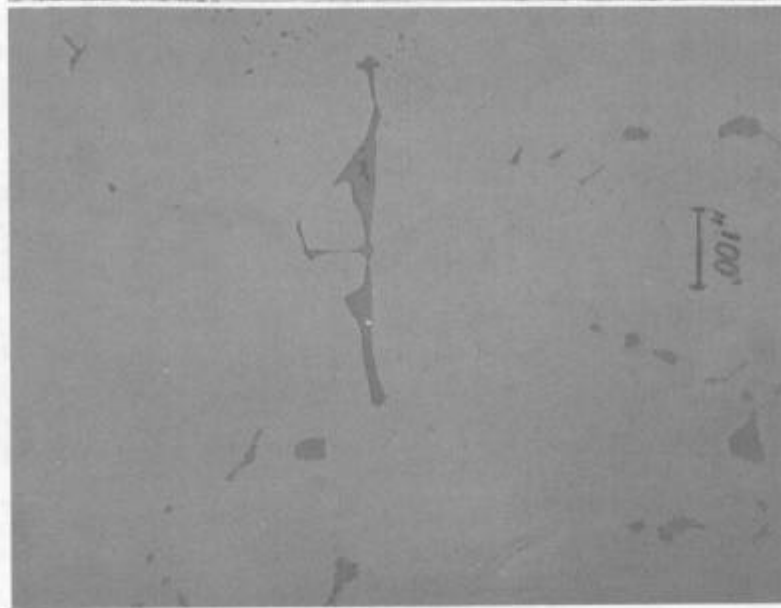


Figure 1. Heat WWS, Mid-radius of blisk, large and small MC carbides. Unetched.



Figure 2. Heat WST, Near rim of blisk. General structure with MC's and eutectic $\gamma - \gamma'$ nodules. Etched.



Figure 3. Same as Fig. 2, higher magnification to show γ' and carbides.

Heat No.	Inspected Area in ²	Defects Found
WLB	1.62	1 dirt stringer 3 mils long
WLK	1.68	1 "hole" 4X10 mils
WST	6.17	2 dirt stringers: 3½ mils; 11 mils long
		2 dirt/dross: 2½X6½ mils; 4 mils dia
WWS	2.93	1 pore or carbide pullout 1½ mil dia
		2 dirt/dross: 1X3½ mils; 2½X5 mils
Total Area	<u>12.5</u> in ²	

The longest linear dimension of a defect was 11 mils for a dirt (oxide?) stringer, Heat WST, Fig. 4. The largest dirt clump was in Heat WWS, Fig. 5. The 10 mil long "hole" was found near the fracture area of a crack growth specimen. This might have been a carbide or dirt area that was opened up by the testing. It did not resemble any kind of normal porosity.

In addition to metallographic examination for defects, one blisk (Heat WWS) was used for the ECM type of successive polishing to detect non-metallic particles. A circular area (4.5 in²) in the hub was inspected. ECM "slices" were taken every 0.020 inch for 92 planes, a total of 414 in². One 5 mil inclusion was found 0.160 inch below the top surface (the poorer surface) and one 8 mil inclusion was found deeper: no others above the limit of detectability (about 2 mils) were found.

The fractographic examination of the LCF and HCF test bars can be summarized as follows. In general, as temperatures increased and stresses and

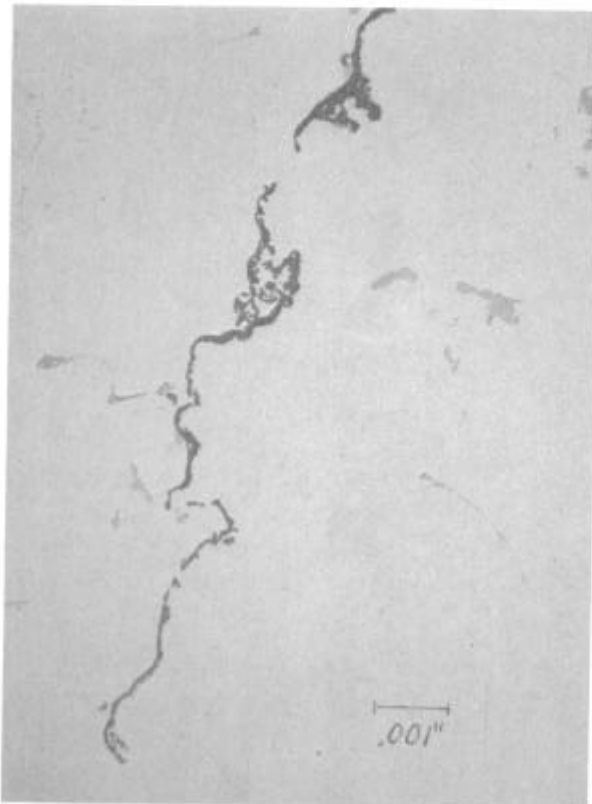


Figure 4. Heat WST. Longest linear inclusion found. Unetched

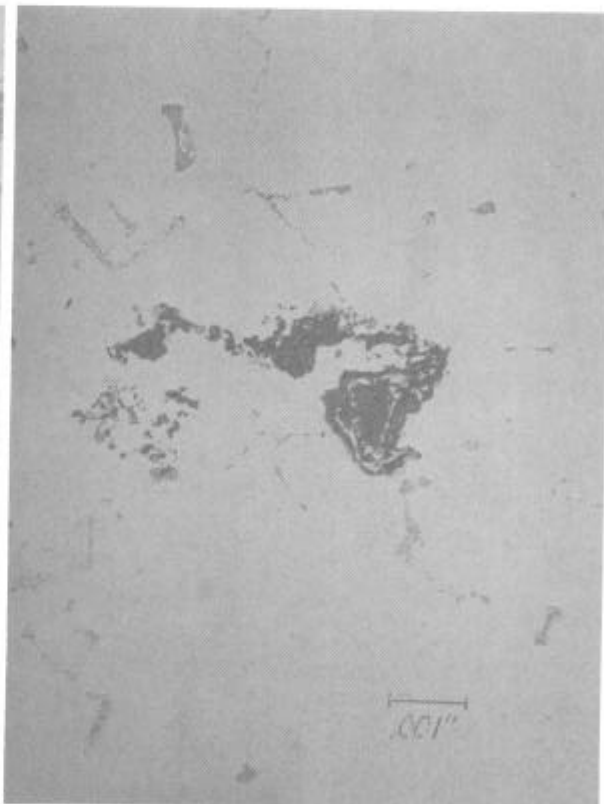


Figure 5. Heat WWS. Largest blocky inclusion found. Unetched

A ratio decreased, there was a tendency for the fracture origin to move from the surface to the interior. No true foreign material defects (rich in Al, Si, etc.) were found. In some cases, there were Hf, Ta, Ti rich spots at the origin. These are most likely MC carbides, which is not unexpected since they are so prevalent in the structure. A few samples had Cr enriched areas, which may have indicated the presence of Cr-containing carbides or dendrite segregation. They did not "glow" in the SEM as oxides would. The presence of facets at the origin area was common for both LCF and HCF specimens.

The fracture surfaces of the four crack growth rate specimens were also examined. No defects were found, but carbides and carbide clusters up to 3 mils were generally present at the initiation locations (MC carbides again verified by EDX analysis).

Discussion

The mechanical properties of Mar-M-247 obtained in the present work are quite similar to those reported for Grainex^(R) cast and HIP material(1)(2). The U.T.S. rises gradually from R.T. to about 1200F before decreasing in agreement with the prior data, and the tensile ductility has the usual minimum near 1500-1600F. Tensile data showed a relatively small scatter, considering the variety of castings and specimen locations involved. This has been attributed to the Grainex^(R) process, which avoids very coarse grains in the thicker sections, and to the HIP, which eliminates virtually all porosity and provides some additional homogenization. Notched/smooth U.T.S. ratios, while not as high as some lower strength cast alloys or wrought alloys, are still probably greater than 1.2 at temperatures under 1200F.

It should be kept in mind that the grain size of most of the test bars was about 1/8" diameter, which is larger than found in normal cast-to-size test bars (1/64-1/16"), and that comparisons with other alloys have to be made on this basis.

The creep and rupture times are as expected and are close to reported values. The rupture ductility at 1400F is low, but at 1600 and 1800F is reasonably good.

Strain controlled LCF properties agreed well with prior data. Scatter in the LCF data is relatively low, again indicative of the effects of grain size control and HIP.

Very little axial-axial HCF data is available for comparison. Somewhat striking is the relatively low $A=\infty$ fatigue strength at 1100F; lower than at 1500 or 1700F. Many nickel-base alloys do show this type of HCF, $A=\infty$ behavior - a peak fatigue strength at some intermediate temperature, with lower strength below and above it.

Crack growth rate data agrees very well with earlier data. At 1000F, the K^* is 8 Ksi $\sqrt{\text{in}}$ and at 1400F is 12. At both temperatures K_{IC} was not reached up to ≥ 50 .

The microstructure of Mar-M-247 was similar in all sections examined, and is as expected for this type of alloy. A major item of interest in the structure is the MC carbide size and morphology, since they are extremely brittle, and undoubtedly can act as crack initiators and possibly easy crack growth paths. The small, blocky particles (only a fraction of a mil in size) are not of great concern, but the elongated forms could affect fatigue and crack behavior. All the data reported here, however, is on material with

ample carbides of this nature and therefore includes their effects. The fatigue origins on many specimens did have Ti/Ta/Hf rich MC particles present. The longest elongated carbides are about 8-10 mils. In considering casting defects (non-metallic inclusions) then, in effect, only those >10 mils are really significant.

Conclusions

1. Mechanical property data for Grainex(R) + HIP Mar-M-247 specimens cut from blisks including tensile, creep rupture, LCF, HCF, and crack growth results indicated that properties and cleanliness confirmed prior information and further indicated that engine applications for this material are feasible.
2. Inspection for defects revealed no porosity, and some non-metallic inclusions up to 11 mils in length.

References

1. "Grainex^(R) Cast Mar-M-247 Alloy," Technical Bulletin TB3000, Howmet Turbine Components Corporation
2. Harris, K. and R. E. Schiver, "Vacuum Induction Refining MM0011 Mar M-247 for High Integrity Turbine Rotating Parts," Cannon-Muskegon Corporation
3. Morrow, Hugh III, "The Effect of Molybdenum Content on the Microstructure and Mechanical Properties of Mar-M 247, a Cast Nickel-Base Superalloy," RP-57-72-04, Research Laboratory, Climax Molybdenum Co. of Michigan. Dec. 14, 1973
4. Nathal, M.V., R.D. Maier and L.J. Ebert, "The Influence of Cobalt on the Tensile and Stress-Rupture Properties of the Nickel-Base Superalloy MAR-M 247," Met. Trans. 13A, Oct. 1982
5. Ibid., "The Influence of Cobalt on the Microstructure of the Nickel-Base Superalloy MAR-M247," Met. Trans. 13A, Oct. 1982